International Journal of Heat and Mass Transfer 135 (2019) 604–613

Contents lists available at ScienceDirect

International Journal of Heat and Mass Transfer

journal homepage: www.elsevier.com/locate/ijhmt

# Theoretical, numerical, and experimental investigation of smoke dynamics in high-rise buildings

Chan-Sol Ahn [a,b,1], Boo-Hyoung Bang [a,c,1], Min-Woo Kim [a], Scott C. James [d], Alexander L. Yarin [e,*], Sam S. Yoon [a,*]

[a] School of Mechanical Engineering, Korea University, Seoul 136-713, Republic of Korea
[b] Fire Research Center, Korea Institute of Civil Engineering and Building Technology, 283, Goyang-daero, Ilsanseo-gu, 10223 Goyang-si, Republic of Korea
[c] Technology Development Team, Daewoo Inst. of Const. Tech., 60, Songjuk-dong, Jangan-gu, 440-210 Suwon, Republic of Korea
[d] Depts. of Geosciences and Mech. Eng., Baylor University, Waco, TX 76798, USA
[e] Department of Mechanical & Industrial Engineering, University of Illinois at Chicago, 842 W. Taylor St., Chicago 60607, USA

ARTICLE INFO

*Article history:*
Received 4 September 2018
Received in revised form 29 November 2018
Accepted 13 December 2018

*Keywords:*
Self-similar turbulent plume
Fire Dynamics Simulator
High-rise buildings
Smoke dynamics

ABSTRACT

Smoke kills more people than the associated fire and thus predicting smoke spreading inside high-rise buildings is of paramount importance to structural and safety engineers. Here, the velocity, temperature, and concentration fields in large-scale turbulent smoke plumes were predicted using classical self-similar turbulent plume theory, which assumes a point fire source under open-air conditions. Turbulent fires of various heat release rates in a confined space were also simulated numerically using Fire Dynamics Simulator (FDS), which was verified against experimental data before being used to validate the analytical plume jet results. The agreement between analytical, numerical, and experimental results was good. This demonstrates for the first time that for realistic, wide shafts, analytical results from self-similar theory of free turbulent plumes are as accurate as the numerical simulations and appropriately describe experimental data. This allows engineers to avoid lengthy, cumbersome numerical simulations to estimate the consequences of smoke spreading in high-rise buildings using simple analytical formulae. In addition, parametric studies were conducted using plume theory for building heights up to 500 m and heat release rates up to 500 MW. Smoke velocity, temperature, and concentration fields described smoke evolution at different heights.



## 1. Introduction

It is well-known that smoke poses a greater danger to life than the associated fire because smoke spreads rapidly through a building. For this reason, smoke dynamics are of paramount importance for structural and safety engineers who design evacuation paths to minimize casualties. Fire detection, heating of the building, smoke-filling rates, and fire ventilation are all features related to the physical properties of the fire. Smoke propagation in a stairwell and long vertical shafts in a closed environment has been extensively studied experimentally and numerically. However, analytical assessment has not yet been attempted [1–14].

Turbulent flame propagation inside a building is an extremely complex phenomenon because the heat-release rate nonlinearly varies as the fire grows [15]. Furthermore, the spreading of smoke is never symmetric because air supply through windows and doors is essentially random while the fire propagates as it grows [16]. Fire dynamics in a complex system (geometry) can be modeled using a fully turbulent 3D fire computational tool like Fire Dynamics Simulator (FDS). However, 3D computations are prohibitively time-consuming and often not useful to safety engineers who demand quick spatio-temporal estimates of smoke velocity, temperature, and concentration as a function of the fire size. Because a quick first estimate is required, simple analytical predictions would be very useful. In this work, we demonstrate to what extend the analytical self-similar semi-empirical theory of turbulent plumes is capable to predict the dynamic characteristics of rising smoke at various fire scales. The source of smoke can be liquid-fuel (e.g., a pool fire), solid-fuel, or gas combustion. The self-similar theory assumes that the smoke source is much smaller than the ventilation shaft or stairwell width and thus, can be considered as a pointwise heat source. Moreover, one can assume that air access to and from the shaft at all floors is practically unlimited (e.g., because of the open doors) and heat losses are minor, which

* Corresponding authors.
*E-mail addresses:* ayarin@uic.edu (A.L. Yarin), skyoon@korea.ac.kr (S.S. Yoon).
[1] These authors have contributed equally.

https://doi.org/10.1016/j.ijheatmasstransfer.2018.12.093
0017-9310/

diminishes the effect of the ventilation shaft or stairwell walls on the plume development even at the higher levels. As a result, the self-similar theory as well as numerical solutions for an open plume represent a plausible first approximation for such high-rise buildings.

Numerous studies of axisymmetric smoke plumes are available [17–21]. These studies assumed Gaussian profiles of velocity and temperature at various axial locations (or heights) in the non-combustion region sufficiently distant from the heat source. Turbulent mixing was modeled assuming momentum transfer at the interface between the rising plume and the entrained air. Morton et al. [21] and Turner [22] developed an approximate theory describing buoyant convection currents above a pointwise heat source based on the so-called entrainment hypothesis. Yokoi [23] applied turbulent boundary layer theory based on the Prandtl mixing length theory and provided a comprehensive study on prevention of fire spread due to hot, buoyant currents. The axial velocity and temperature scale with varying heat release rate ($Q_z$) and height ($L$) were predicted. Morton et al. [24] later extended "weak" plume theory to include "strong" plume effects; here weak plume theory assumed a point heat source while the strong plume theory considered the geometry (length and height) of the heat source. Heskestad [25] noted that the theory of Morton et al. [24] was valid for both weak [23,26] and strong plumes [27–29] with some modification. Heskestad [30] also predicted smoke mass flowrates as a function of elevation and with air entrained at lower elevations. Quintiere [31] provided scaling laws for fires using dimensionless groups derived from the governing equations. Quintiere and Grove [32] presented a unified model that distinguished the "near-field" combustion and "far-field" zones for a point heat source. All these plume models indicated that the smoke centerline temperature ($\Delta T = T_L - T_\infty$) scaled as $\Delta T \propto Q_z^{2/3} L^{-5/3}$ while the smoke centerline velocity ($u_{\max}$) scaled as $u_{\max} \propto Q_z^{1/3} L^{-1/3}$. Sun et al. [4] used these scales to model smoke rise in a shaft caused by a compartment fire. With some adjustable constants, it is reasonable to use plume theory to model smoke spread in a confined area. A relevant comprehensive review on fire dynamics in high-rise buildings is available in Sun et al. [4]. Oka and Oka [20] used FDS to model an oscillating-plume fire and provided the corresponding modified scaling law for $\Delta T$.

The theory of self-similar, laminar plane and axisymmetric plumes developed by Zeldovich [33] laid the foundation for this field. This jet theory is a part of the general boundary layer theory of buoyancy-driven flows described in the well-known monographs of Jaluria [34] and Yarin [35], as well as in the review of Turner [22]. Self-similar solutions for turbulent plane and axisymmetric plumes in the context of the turbulent Prandtl mixing-length theory are available [35]. The self-similar turbulent-plume theory provides analytical solutions for the velocity, temperature, and smoke-concentration fields as well as the flowrate of a rising plume in the axial direction for a wide range of heights and fire strengths. This theory holds great promise for predicting building fires and smoke spreading to various heights. Nevertheless, these results stay practically unknown to safety engineers, and still had found no applications in their practice. One of the reasons for such unsatisfactory state of the art is probably related to the fact that the idealized assumptions of the self-similar theory have never been tested in comparison with realistic smoke plumes arising in confined shafts. Only such a comparison could help to evaluate the practical strength and limitations of the self-similar analytical theory, to ascertain its range of validity under realistic practical conditions, and thus facilitate its wide introduction in the safety engineering practice. Here, for this aim, the analytical predictions of the self-similar turbulent plume theory were compared to FDS simulations as well as experimental data, and their wide range of validity was established.

## 2. Theoretical, numerical, and experimental methods

### 2.1. Plume jet theory

In the boundary layer theory of turbulent plumes, as usual, the velocity at the asymptotic lateral boundary of the plume is zero, and thus there is no convective heat loss through the boundary at all (cf. [35]). Also, the conductive heat flux is zero [35]. These boundary conditions are realistic as far as the plume does not experience a significant interaction with the ventilation shaft or stairwell walls. For the case of high-rise buildings, such situations are possible, namely, when air access to and from the shaft at all floors is practically unlimited (e.g., because of the open doors), and lateral heat losses are minor.

According to Yarin [35] for the axisymmetric case of primary interest here, the most important parameter governing smoke spread in turbulent plume is the released power $Q_z$ or its counterpart $Q_r = Q_z/(\rho c)$ where $\rho$ and $c$ are the gas density and specific heat at constant pressure, respectively [35]. For an axisymmetric plume:

$$Q_r = \int_0^\infty u(T - T_\infty) r \mathrm{d}r, \tag{1}$$

where $u$ is the longitudinal velocity profile along the plume, $T$ is the temperature distribution in the plume, $T_\infty$ is the temperature of the surrounding gas, and $r$ is the radial coordinate in any plume cross-section reckoned from the plume axis (the vertical $z$ axis *here*). It should be emphasized that the value of $Q_r$ (and obviously $Q_z$) is always a specified parameter, which is invariant along the plume. Note also that in the present case both values were divided by $2\pi$.

The maximal longitudinal velocity along the rising plume is $u_{\max}$. In a turbulent axially symmetric plume it is equal to [Yarin [35], the first Eq. (6.111)]:

$$u_{\max}(z) = \left(\frac{\beta g Q_z}{\rho c z}\right)^{1/3}, \tag{2}$$

where $\beta$ is the thermal expansion coefficient of gas, and $g$ is gravity acceleration.

For a building height of $z = L$, the preceding equation yields the buoyancy-driven velocity at the top of the building:

$$u_{\mathrm{top}} = \left(\frac{\beta g Q_z}{\rho c L}\right)^{1/3}. \tag{3}$$

Similarly, the axial (maximal in cross-section) temperature in such a plume is [Yarin [35], with a misprint in the second Eq. (6.111) corrected]:

$$T_{\max}(z) - T_\infty = \left(\frac{Q_z}{\rho c}\right)^{2/3} \frac{1}{(\beta g)^{1/3}} \frac{1}{z^{5/3}}. \tag{4}$$

Accordingly, the temperature of the gas-carrying smoke at the building top is:

$$T_L - T_\infty = \left(\frac{Q_z}{\rho c}\right)^{2/3} \frac{1}{(\beta g)^{1/3}} \frac{1}{L^{5/3}}. \tag{5}$$

Note also that the smoke concentration, $C$, and excess temperature, $T - T_\infty$, satisfy identical equations (because the eddy thermal and mass diffusivities are essentially equal) and have identical boundary conditions. Therefore, the dependence $C \sim z^{-5/3}$ is expected for the maximal concentration in the rising turbulent plume.

It is instructive to compare the above-mentioned classical results to those from fire-fighting literature. Sun et al. [[36], Eq. (31)] stated that:

$$u_{top} \propto Q_z^{1/3}, \tag{6}$$

in full agreement with the scaling predicted by (3).

Also, Sun et al. [[4], Eq. (5)] showed that:

$$T_L - T_\infty \propto Q_z^{2/3} \frac{1}{L^{5/3}}, \tag{7}$$

in full agreement with the scaling law predicted by (5). Accordingly, the results used in the fire-fighting literature are in full agreement with the preceding results from the hydrodynamic and heat-transfer theories.

It should be emphasized that the fire-fighting literature attributes these results to particular considerations, whereas they follow from the basic theory of turbulent, buoyant plumes, which demonstrates that the latter are indeed a relevant generic model for rising compartment fires in building shafts.

If a shaft allows for unimpeded air entrainment into a rising plume from intermediate floors, then the volumetric flow rate in the shaft will increase similarly to a free plume (divided by $2\pi$):

$$\dot{Q} = \int_0^\infty ur\mathrm{d}r. \tag{8}$$

Accordingly, the self-similar solution yields:

$$\dot{Q} = \left(\frac{\beta g Q_z}{\rho c z}\right)^{1/3} z^2 \times \text{constant}, \tag{9}$$

Therefore, the volumetric flow rate through the shaft top $\dot{Q}_{top}$ is found as

$$\dot{Q}_{top} = \left(\frac{\beta g Q_z}{\rho c}\right)^{1/3} L^{5/3} \times \text{constant}, \tag{10}$$

At the top where $z = L$, smoke concentration decreases relative to the ground floor as $L^{-5/3}$.

Note also that (3) and (5) can be re-written in dimensionless form:

$$Re_{top} = Gr_{top}^{1/3} \left[\frac{Q_z}{\nu(T_{top} - T_\infty)\rho c L}\right]^{1/3}, \tag{11}$$

where the Reynolds and Grashof numbers are, respectively:

$$Re_{top} = \frac{u_{top} L}{\nu}, \quad Gr_{top} = \frac{\beta g (T_{top} - T_\infty) L^3}{\nu^2}, \tag{12}$$

with $\nu$ being the kinematic viscosity of gas.

### 2.2. Fire Dynamics Simulator (FDS)

FDS is a computational tool based on the Navier-Stokes equations appropriate for low-speed (Ma < 0.3), thermally-driven smoke originating from fires. Turbulence is modeled using large eddy simulation (LES). Combustion is modeled through a mixture-fraction analysis that presumes immediate reaction of fuel and oxygen. Radiation transport is based on a non-scattering gray gas and a wide-band model. The governing equations include continuity, species concentration balance, momentum and energy balances, and the ideal gas law [37]:

$$\frac{\partial \rho}{\partial t} + \nabla \cdot (\rho \mathbf{u}) = 0, \tag{13}$$

$$\frac{\partial \rho Y_\alpha}{\partial t} + \nabla \cdot (\rho Y_\alpha \mathbf{u}) = \nabla \cdot (\rho D_\alpha \nabla Y_\alpha) + \dot{m}_\alpha''', \tag{14}$$

$$\frac{\partial \rho \mathbf{u}}{\partial t} + \nabla \cdot (\rho \mathbf{u}\mathbf{u}) = -\nabla \tilde{p} - \nabla \cdot \boldsymbol{\tau} + (\rho - \rho_0)\mathbf{g}, \tag{15}$$

$$\frac{\partial \rho h_s}{\partial t} + \nabla \cdot (\rho h_s \mathbf{u}) = \frac{\mathrm{D}\tilde{p}}{\mathrm{D}t} + \dot{q}''' - \nabla \cdot \dot{\mathbf{q}}'', \tag{16}$$

$$\rho = \frac{\tilde{p}\bar{W}}{RT}, \tag{17}$$

where $D_\alpha$ is the turbulent diffusion coefficient of species $\alpha$, $\mathbf{g}$ is the gravity acceleration vector, $h_s$ is the mass-weighted average enthalpy of the lumped species [38], $\dot{m}_\alpha'''$ is the mass-production rate per unit volume of species $\alpha$ by chemical reaction, $\tilde{p}$ is the pressure perturbation, $\dot{q}'''$ is the heat release rate per unit volume, $\dot{\mathbf{q}}''$ is the heat flux vector, $R$ is the universal gas constant, $t$ is time, $\mathbf{u}$ is the velocity vector, $\bar{W}$ is the molecular weight of the gas mixture, and $Y_\alpha$ is the mass fraction of species $\alpha$. The adiabatic no-slip wall boundary condition is assigned at the bottom surface and an open freestream boundary condition is used for the rest of the outer surfaces.

### 2.3. Experimental

A Joule heater was placed to induce a rising air inside an exit nozzle, which was attached at the top of a smoke cylindrical chamber. The heating power was controlled by an AC regulator, which was between 4.5 and 220 W, depending on the applied voltage. Buoyant smoke was produced by burning incense and was injected through a smoke nozzle to an open-air environment. Buoyancy increased with increasing heating power. Thermocouples (Almemo FVAD 35 TH5Kx, Ahlborn, Germany) were placed at the axial locations of $z$ = 0.3, 0.4, 0.5, 0.6, 0.7, 0.8, 0.9 and 1 m. All temperature and velocity measurements were acquired along the centerline to capture the maximum velocity and temperature. An electric heating coil was situated inside a 3-cm-long, 4-cm-diameter nozzle connected to a chamber containing burning incense. Heat from the burning incense was negligible compared to the supplied power of $32 \le Q_z \le 220$ W. Upon setting the heating power, 15 min was allowed to establish a steady state prior to measurements. Each test was repeated thrice and the results were averaged to yield the final temperatures and velocities. The ambient air temperature was $T_\infty$ = 24 °C with the relative humidity level of about 30%.

## 3. Results and discussion

### 3.1. Code verification

A grid-convergence study was carried out for a $CH_4$ fire of $Q_z$ = 1 MW in a Cartesian domain of $7 \times 7 \times 40$ m$^3$ with grid resolutions of $80 \times 80 \times 175$ (1.12 M nodes), $80 \times 80 \times 350$ (2.24 M nodes), $80 \times 80 \times 700$ (4.48 M nodes), and $80 \times 80 \times 1400$ (8.96 M nodes). Rectangular grids were used in the $x$ and $y$ directions with the smallest $\Delta x = \Delta y$ = 0.05 m at the center and the largest $\Delta x = \Delta y$ = 0.3 m near the edges. In the axial direction ($z$), the finest resolution was $\Delta z$ = 0.05 m increasing to $\Delta z$ = 0.1, 0.2, and 0.4 m for the grid-convergence study. All data were acquired at the centerline at the axial location of $z$ = 10 m. All simulations were conducted for $t$ = 100 s and the predicated time-series variations of $u_{max}$, $T_{max}$, and volumetric flowrate, $\dot{Q}$ are compared in Fig. 1. The bottom surface of the domain was treated as an insulating wall and there was no heat flux across the wall. The five remaining surfaces were assigned open-air conditions. The simulations revealed that this was applicable when the shaft was sufficiently large, i.e., a bottom area of 1600 m$^2$. Air temperature and pressure were initially set to $T_\infty$ = 20 °C and $P_\infty$ = 1 bar.

Fig. 1 compares the numerical results for $u_{max}$, $T_{max}$, and $\dot{Q}$ for grid resolutions of $\Delta z$ = 0.05, 0.1, 0.2, and 0.4 m. Both $u_{max}$ and $T_{max}$ were under-predicted using the coarsest grid ($\Delta z$ = 0.4 m) because

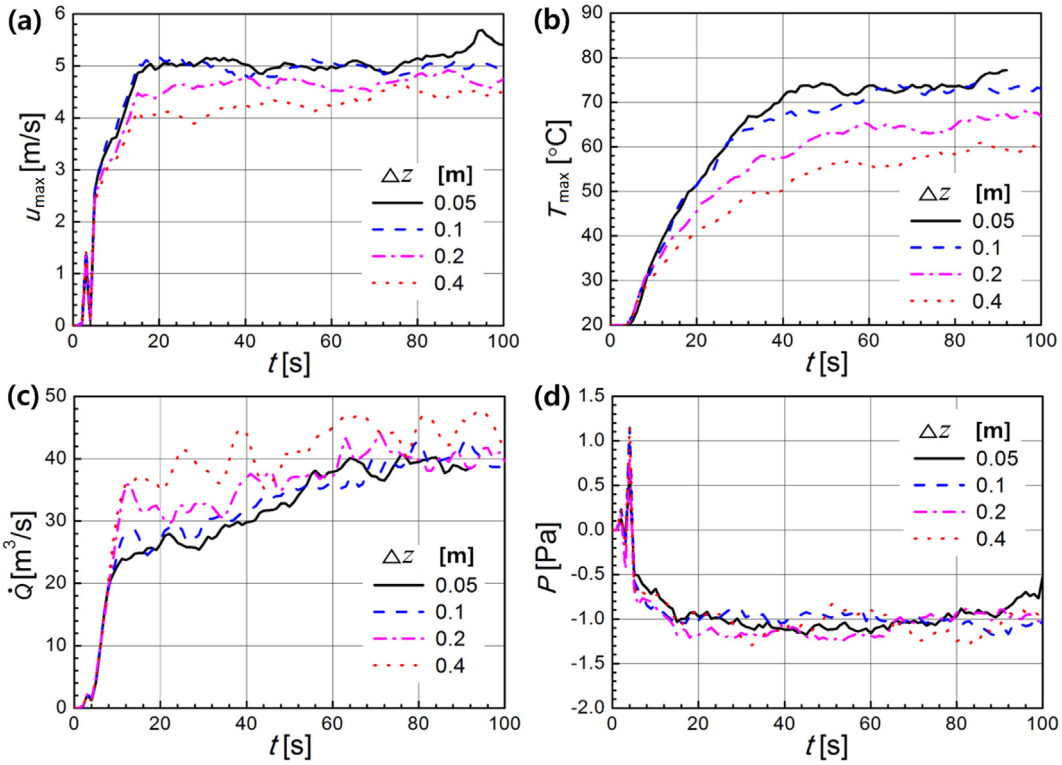


**Fig. 1.** Grid resolution test results for (a) $u_{max}$, (b) $T_{max}$, (c) $\dot{Q}$, and (d) pressure at $z$ = 10 m. A methane flame delivered 1 MW at $z$ = 0 m. The initial temperature was $T_\infty$ = 20 °C.

insufficient resolution smeared out detailed information, which in turn reduced the overall $u_{max}$ and $T_{max}$ values. Both $u_{max}$ and $T_{max}$ converged for $\Delta z = 0.05$ and 0.1 m, so the grid resolution of $\Delta z = 0.1$ m was selected. For $\dot{Q}$, the coarsest grid with $\Delta z = 0.4$ m yielded the largest fluctuations and magnitude while convergence was demonstrated at $\Delta z = 0.05$ and 0.1 m. As evident in Fig. 1d, pressure was not sensitive to grid resolution.

### 3.2. Code validation

Prior to comparing the FDS predictions to the analytical self-similar plume theory, the model was verified using the experimental data of Sun et al. [4]. Fig. 2 depicts the experimental setup testing compartment gasoline fires in a confined shaft. The dimensions in Fig. 2 are the same as those specified by Sun et al. [4]. Air was supplied through an open door located at the bottom left spreading the flame to the right, while smoke spread through the shaft as shown in Fig. 2. All snapshots in Fig. 2 correspond to a quasi-steady state where most quantities fluctuated minimally.

The compartment within which the gasoline pool fire was located had dimension $0.7 \times 0.3 \times 0.4$ m$^3$ while the shaft height was 2.4 m ($70 \times 30 \times 240$ nodes). The open door located at the bottom left wall had dimensions $0.12 \times 0.18$ m$^2$. An open window at the top left of the shaft top was a square with an area of 0.015 m$^2$. The heating power $Q_z$ of the gasoline fire was the product of the fuel burning rate ($4.31 \times 10^{-5}$ kg/s) and the lower heat value of the fuel ($4.7 \times 10^4$ kJ/kg). Sun et al. [4] recorded time-series variations in $\Delta T$ at the axial locations of $z$ = 0.1, 0.3, 0.55, 0.9, 1.22, 1.55, 1.88, and 2.22 m using K-type (Ni-Cr/Ni-Si) thermocouples [4], which are compared to FDS simulations in Fig. 3. The histories of

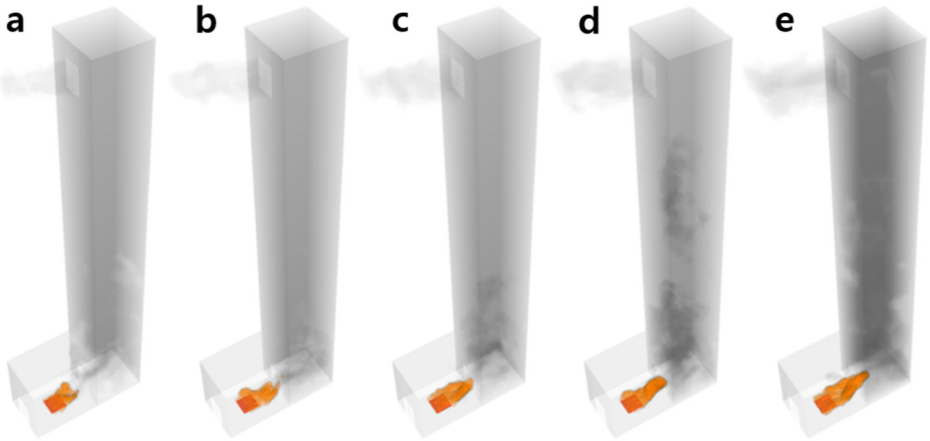


**Fig. 2.** Gasoline fire snapshots and smoke dynamics at a quasi-steady state in a confined shaft for various values of $Q_z$: (a) 2.0, (b) 2.7, (c) 3.6, (d) 4.5, and (e) 5.5 kW.

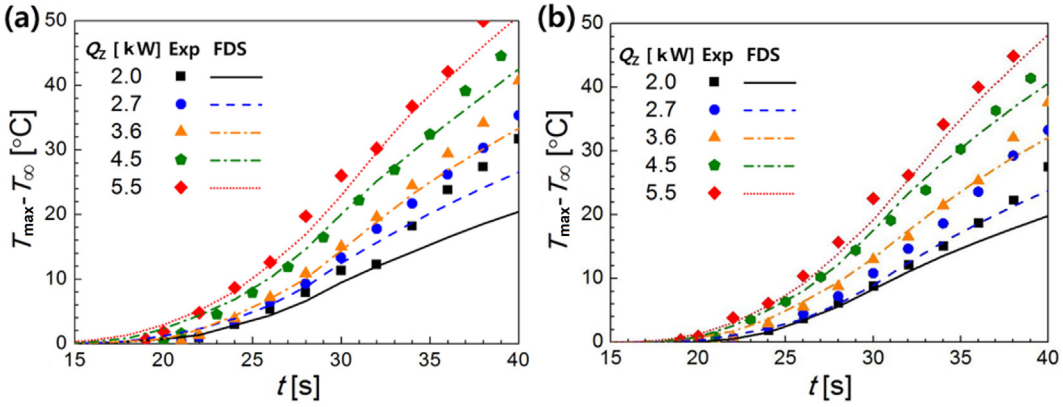


**Fig. 3.** Centerline temperature histories with varying values of $Q_z$ of gasoline pool fires at $z$ = (a) 0.9 and (b) 1.55 m.

centerline gas temperatures ($\Delta T = T_{max} - T_\infty$) were compared for various values of $Q_z$ at $z$ = 0.9 and 1.55 m in Fig. 3a and b, respectively. The greater is the value of $Q_z$, the greater is the centerline temperature $\Delta T$, in both the experiment and the corresponding FDS simulations. The rate of $\Delta T$ increase also agreed between the experiment and FDS simulations although minor deviations were evident in some cases. As expected, $\Delta T$ decreased with axial distance as smoke moved away from the fire source. Cooler smoke at higher elevations was attributed to smoke dilution, energy losses to walls, and the elevation changes. The $\Delta T$ reduction with the increasing $z$ was evident in both the experiment and the corresponding FDS simulations in Fig. 3a and b.

It is noted that FDS simulations tended to deviate from the experimental data as time increased, especially at lower values of $Q_z$ (cf. Fig. 3). This deviation decreased for larger values of $z$. FDS tended to under-predict temperatures when heating power was low and heat transfer between computational cells was fairly small. This shortcoming of FDS was due to the approximations involved in the sub-grid-scale (SGS) isotropic turbulence formulation. The SGS turbulence model was reasonably accurate for larger fires, but less accurate for small fires. Turbulence is more likely to be isotropic for large fires, but may have a preferred direction for small fires. Nevertheless, considering FDS simulations as the whole, the computational resolution was satisfactory.

Fig. 4a and b show cross-sectional fields of $u$ and $T$ during the development stage of the fire at $t$ = 24 s for various values of $Q_z$ in gasoline pool fires. Fig. 4c and d show the time-averaged results for the velocity vectors and smoke streamlines. Increasing $Q_z$ accelerates smoke spreading because of the corresponding increase in burning rate and air influx. As a result, as $Q_z$ increases, $u$ increases both at the inlet (bottom) and outlet (top) as shown in Fig. 4. In Fig. 4b, higher temperature zones in the compartment ceiling and the shaft on the right were observed as $Q_z$ increased. A recirculation zone formed near the compartment ceiling, trapping hot air

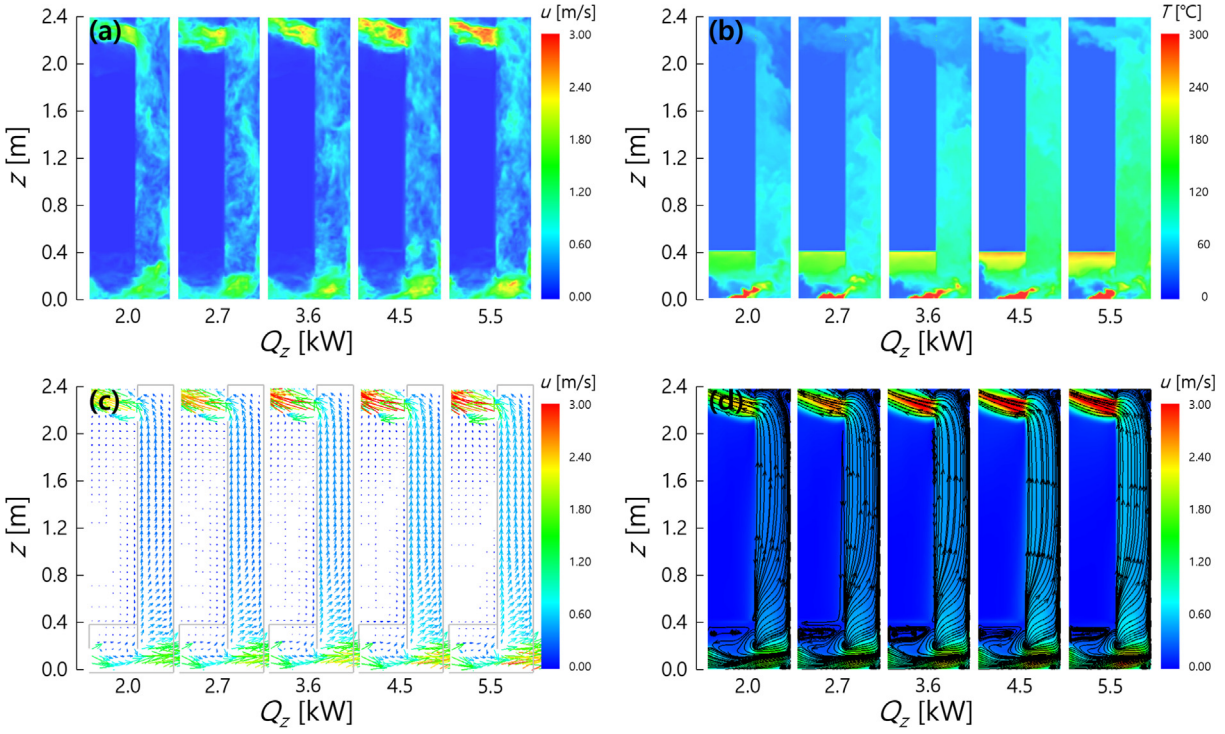


**Fig. 4.** Effect of $Q_z$ on $u$ and $T$ on gasoline pool fires. Cross-sectional fields of (a) $u$ and (b) $T$ during the development stage of the fire at $t$ = 24 s. Time-averaged (c) velocity vectors and (d) streamlines.

as illustrated by the streatmlines in Fig. 4d. Note that air temperature reached a maximum of 400 °C, but the contour limit was 300 °C for clearer presentation.

A qualitative comparision was made between experimental images and FDS temperature contour results in Fig. 5a and b, respectively. Heating power was varied from 4.5 to 220 W to observe effects on smoke dynamics as a function of buoyancy. The experimental images in Fig. 5a show laminar behavior when smoke exited the nozzle. Smoke flow was laminarized through a converging nozzle that suppressed small-scale turbulent eddies. However, when smoke was injected into open air, turbulence quickly developed and grew with distance downstream. Such laminization was also encountered in the FDS simulations. Overall, the comparision is good because turbulence increased with heating in both the simulations and experiments.

Fig. 6 compares the experimental data and FDS numerical results. In Fig. 6a, the maximum temperature at the centerline in the axial direction ($z$) is compared. As the results show, the greater heat flux value ($Q_z$) results in a higher temperature of the rising air. Fig. 6b also shows that the greater $Q_z$ results in a higher centerline axial velocity ($u_{max}$) of the rising air, which indicates a stronger buoyancy at an increased $Q_z$. The FDS numerical simulations also show consistent trends for both $T_{max}$ and $u_{max}$. The axial temperature $T_{max}$ decreases along the plume because of the air entrainment and lateral heat losses. The longitudinal axial velocity $u_{max}$ also decreases as the plume jet profile flattens because of the air entrainment and friction at the side walls. Based on the fact that both $T_{max}$ and $u_{max}$ are well predicted by FDS simulations, it is reasonable to believe that the accuracy of the rest of the FDS results is well assured.

### 3.3. Effect of heat release rates at various heights

It should be emphasized that the self-similar theory of buoyant plumes employed here is valid when the size of the heat source and the lateral plume size are significantly smaller than the lateral size of the confinement. For some of the high-rise buildings this is a plausible assumption. For this reason, below the numerical simulations and theoretical predictions are based on the open-air environment.

A parametric study was performed for $1 \leq Q_z \leq 100$ MW for a $CH_4$ fire under the open conditions. Both FDS and analytical self-

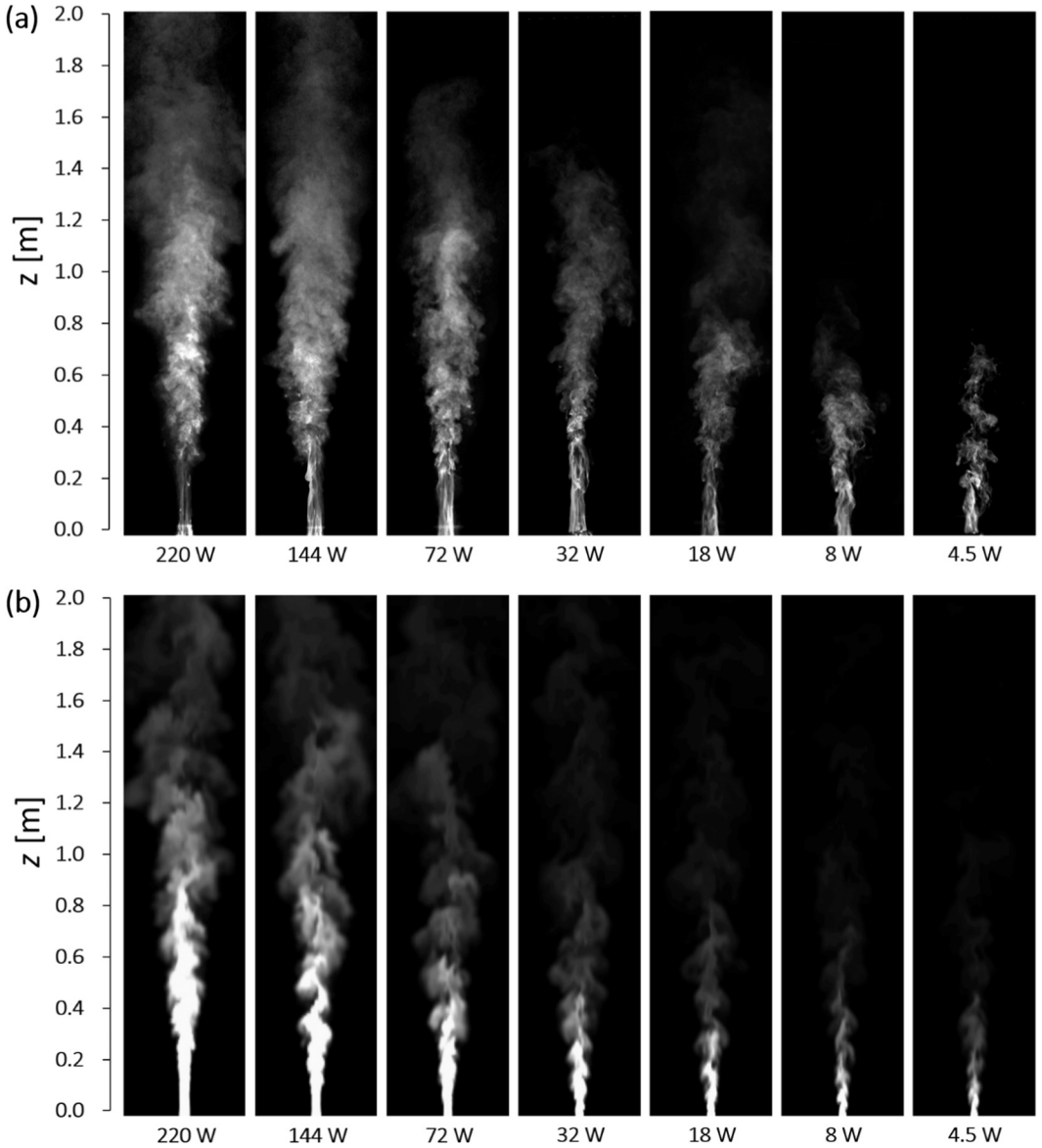


**Fig. 5.** Comparision of smoke flow in (a) experiments and (b) simulations for $Q_z$ varying from 4.5 to 220 W.

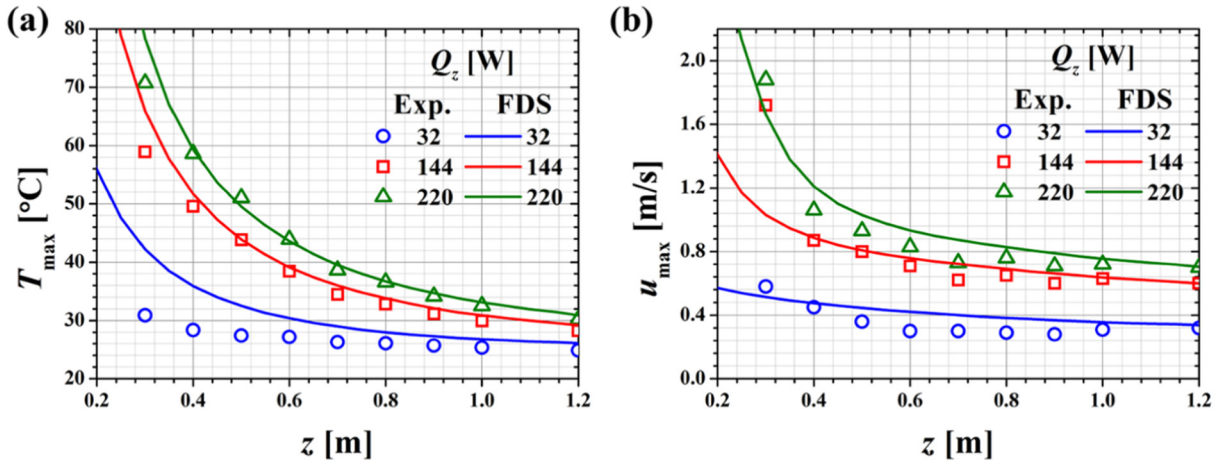


**Fig. 6.** Comparision between the experiments and FDS numerical simulations for (a) $T_{max}$ and (b) $u_{max}$ for $32 \le Q_z \le 220$ W.

similar plume theory predicted centerline $u$ and $T$ distributions, as well as $\dot{Q}$. Theoretical predictions from plume theory were calculated using (2), (4), and (9). The computational domain was $36 \times 36 \times 105$ m$^3$ with $120 \times 120 \times 1050$ (~15 M) nodes. The finest grid resolution of $\Delta x = \Delta y = 0.05$ m was along the centerline with outwardly coarsening resolution. In the axial direction, $\Delta z = 0.1$ m based on the grid-convergence study. The thermophysical properties of $CH_4$ were from Span and Wagner [39]. A single-step reaction was assumed for combustion products:

$$CH_4 + 2O_2 + 7.52N_2 \rightarrow CO_2 + 2H_2O + 7.52N_2. \quad (18)$$

Fig. 7 shows snapshots of the 200-kW/m$^3$ iso-surface of the heat release rate per unit volume (HRR) of the $CH_4$ fires for $Q_z$ = 1–100 MW. A periodic "puff cycle" always initiated at the bottom of the plume. Desjardin et al. [40] explained that such puffing was due to mismatch in the vertical pressure and radial density gradients, which yielded a localized torque. Puffing instabilities entrain fresh air into the fire reinforcing the toroidal vortex motion. This vortex motion spreads in the azimuthal (circumferential) direction, forming finger-like instabilities, the details of which were captured by the FDS simulation for large fires ($Q_z \ge 20$ MW).

Fig. 8a and b show the FDS-simulated gas velocity $u$ and temperature $T$ distributions at the centerline where these values are maximal. Because these fires are in an open-air setting, air is continuously entrained, which is augmented by the natural puffing cycle. Along the axial direction, $u$ decreased as the plume entrained more air. Similarly, $T$ decreased axially upon entrainment of cooler air. As the plume widened, the thermal energy was redistributed radially and the overall temperatures decreased. For $Q_z$ = 100 MW, pockets of air as hot as the bottom of the flame were captured due to cyclic puffing as evident in Fig. 8b.

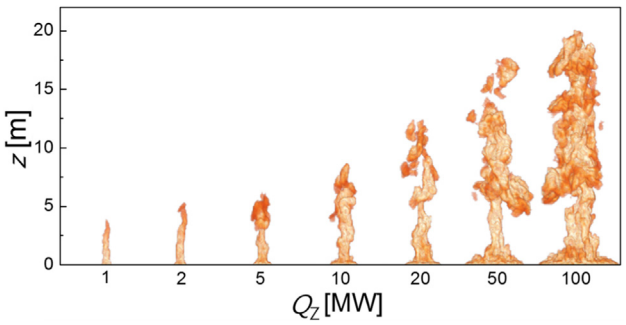


**Fig. 7.** Snapshots of the $CH_4$ fire from the FDS simulations showing iso-surfaces of HRR for $Q_z$ = 1–100 MW.

Fig. 8c reveals a fairly good agreement between the analytical self-similar plume theory and FDS simulations for $u$ for all values of $Q_z$. Note that factors of 3.8, 6.4, and 0.15 were used for the analytical predictions of $u_{max}$, $\Delta T$ ($T_{max} - T_\infty$), and $\dot{Q}$ when comparing to the FDS results; this was equivalent to the introduction of the plume polar distances [4,41]. For all cases, $u_{max}$ decreased with axial distance; $u_{max} \propto L^{-1/3}$. As $Q_z$ increased, $u_{max}$ increased because $u_{max}$ is proportional to $Q_z^{1/3}$ according to (2). In Fig. 8d, $\Delta T$ decreased dramatically in the axial direction because $\Delta T \propto L^{-5/3}$. Naturally, $\Delta T$ was higher when $Q_z$ was larger. Overall, comparison between the analytical theory and FDS was excellent for all values of $Q_z$ and the agreement improved with increasing $z$ because the point-source fire assumption became more appropriate. Fig. 9a also compares predictions from the theory and FDS revealing an increase in $\dot{Q}$ with $z$. The greater the value of $Q_z$, the greater is $\dot{Q}$.

Fig. 9a and b show the effects of $Q_z$ and z on $\dot{Q}$ in a wide range of $Q_z$ variation up to $Q_z$ = 500 MW at axial locations up to $z$ = 500 m. Fig. 9a reveals that the analytical theory performed as good as FDS; therefore, it can be used to reliably predict entrained air flux $\dot{Q}$ for high-rise buildings up to 500 m for various fire strengths. It should be emphasized that Fig. 9a compares the self-similar theory to FDS simulations at steady state. The agreement improved as $Q_z$ increased. The self-similar plume theory assumes a pointwise source and is thus more accurate at greater distances from the source. This situation is typically realized in large-scale problems where the fire source is much smaller than the building scale, whereas the fire power is high resulting in rising smoke at large distances.

The theoretical calculations for $u$ and $\Delta T$ for $2 \le Q_z \le 500$ MW and $1 \le z \le 500$ m from (2) and (4) are plotted in Fig. 9c and 9d. For a fire strength of $Q_z$ = 2 MW and the building height $L$ = 10 m, the smoke velocity at the building top was $u_{max}$ = 6 m/s. For a fire strength of $Q_z$ = 20 MW and the building height $L$ = 100 m, smoke exit velocity was also $u_{max}$ = 6 m/s, which was expected because the axial velocity was constant for a constant ratio of the fire strength to height ($Q_z/L$ is constant). This notion was confirmed when $Q_z$ changed from 5 to 500 MW and the height changed from $L$ = 1 to 100 m; for $Q_z/L$ = 100, the smoke exit velocity remained constant at $u_{max}$ = 18 m/s

This type of ratio analysis can be extended to $\Delta T$ and smoke concentration, $C$. According to (3), modeling the hydrodynamics of buoyant flow in the shaft is possible when $Q_z$ increased proportionally to $L$ [when replacing a high-rise building with a smaller prototype but requiring that experimental and model velocities at the top were the same, i.e. $u_1 = u_2$ from (3)]; i.e., when $Q_z$ /$L$ is

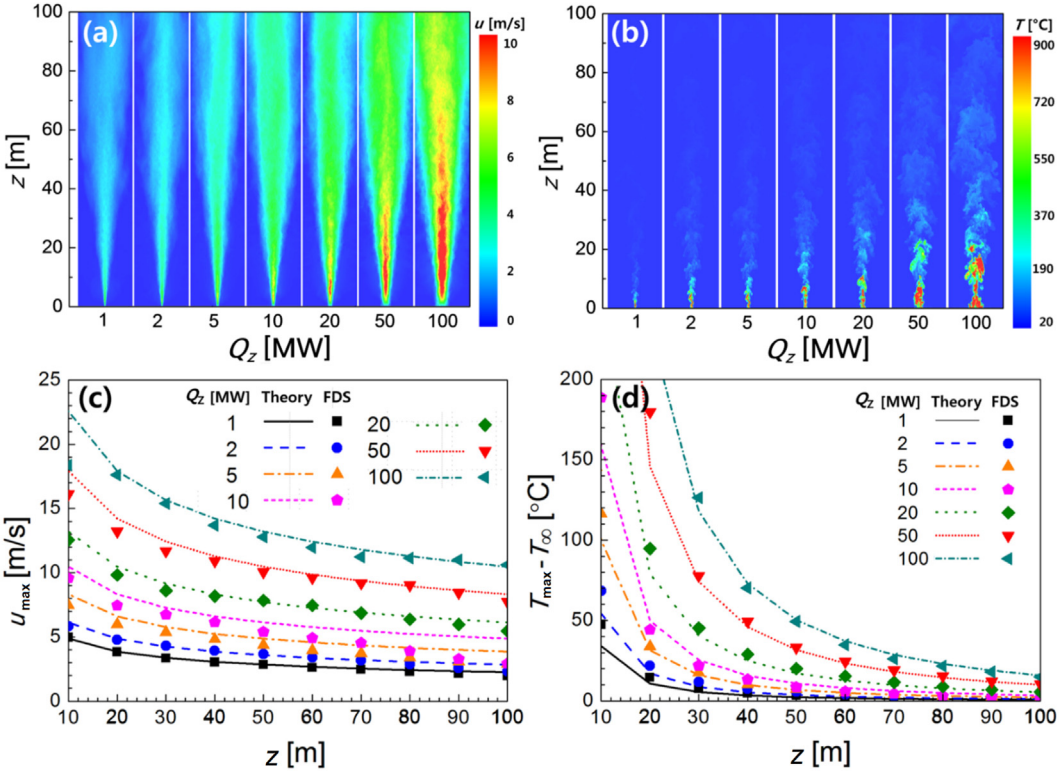


**Fig. 8.** FDS simulations of (a) $u$ and (b) $T$ fields for various $Q_z$. Comparison between the FDS results and the theoretical predictions for (c) $u_{max}$ and (d) $\Delta T_{max}$ for various $Q_z$.

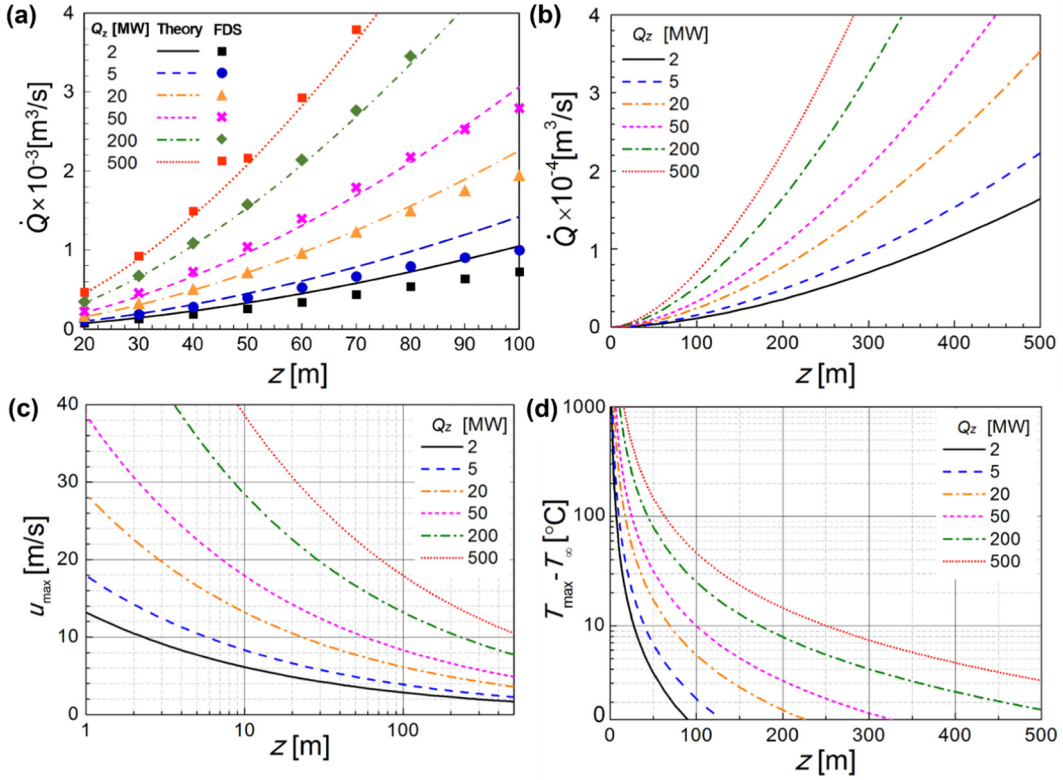


**Fig. 9.** (a) Comparison between the analytical theory and FDS for $\dot{Q}$ corresponding to $2 \le Q_z \le 500$ MW. Parametric studies for: (b) $\dot{Q}$, (c) $u_{max}$, and (d) $\Delta T_{max}$ predicted using the plume theory for $2 \le Q_z \le 500$ MW and $1 \le z \le 500$ m.

a constant. From (5), $\Delta T \propto Q_z^{2/3} L^{-5/3}$, which is proportional to $L^{-1}$ because $Q_z \propto L$; thus $\Delta TL$ is a constant, or $\Delta T_1 L_1 = \Delta T_2 L_2$. Likewise, from (10), $\dot{Q} \propto Q_z^{2/3} L^{5/3}$. Because $Q_z \propto L$, then $\dot{Q} \propto L^{7/3}$. Because $C \propto \dot{Q}^{-1}$, $C \propto L^{-7/3}$ or $CL^{7/3}$ was constant, namely, $C_1 L_1^{7/3} = C_2 L_2^{7/3}$.

On the other hand, a model can specify that $\Delta T$ is constant, i.e., $\Delta T_1 = \Delta T_2$. In such a case, from (5), $\Delta T \propto Q_z^{2/3} L^{-5/3}$. Then, $(Q_z^{2/3}/L^{5/3})_1 = (Q_z^{2/3}/L^{5/3})_2$ or $(Q_{z,1}/Q_{z,2})^{2/3} = (L_1/L_2)^{5/3}$, which can be expressed as $(Q_{z,1}/Q_{z,2}) = (L_1/L_2)^{5/2}$. Thus, $Q_z/L^{5/2}$ is a constant or $Q_z \propto L^{5/2}$. For example, if the length-scale ratio is 2, then the ratio of the heat release rates would be $2^{5/2}$. In other words, if the length scale is doubled, then the fire strength needs to be increased by $2^{5/2}$ or 5.7 to satisfy $\Delta T_1 = \Delta T_2$. Certainly, this is a more difficult condition to satisfy in practice compared to the enforcement of $u_1 = u_2$ discussed in the previous paragraph because of the more stringent enhancement required for $Q_z$. For the previous condition of $u_1 = u_2$, doubling $L$ requires only doubling of $Q_z$.

Fig. 9d illustrates that these scaling laws are in agreement with the predictions made by (3) and (5). For example, if $\Delta T_1 = \Delta T_2 = 8\,^{\circ}\mathrm{C}$ in Fig. 9d, $Q_{z,1} = 2$ MW and $Q_{z,2} = 20$ MW. The corresponding length scales are $L_1 = 2$ m and $L_2 = 5$ m. Here, $L_2/L_1 = 2.5$ and the corresponding heating power ratio should be $Q_{z,2}/Q_{z,1} = (L_2/L_1)^{5/2} = (2.5)^{5/2} = 9.88$, which was close to the heating power ratio of $Q_{z,2}/Q_{z,1} = 20$ MW/2 MW = 10.

## 4. Conclusion

The self-similar turbulent plume theory was used to predict the centerline velocity and temperature $u_{max}$, $\Delta T_{max}$, respectively and the volumetric flow rate $\dot{Q}$ of rising smoke for different fire strengths $Q_z$ and building heights $L$. These theoretical predictions were verified against FDS simulations. The FDS solution was also verified through a grid-convergence study and by comparison to experimental data. While FDS provided transitional details for fire development, quasi-steady state solutions can be quickly obtained using theoretical estimates of $u_{max}$, $\Delta T_{max}$, and $\dot{Q}$. The main result of this work is that under the conditions of a sufficiently wide (but realistic) shaft with free air access, the free plume theory is capable of accurately describing the numerical and experimental data, which means that friction losses at the wall and other confinement effects are minor. These results provide engineers a tremendously power analytical tool for analysis of such situations avoiding cumbersome and lengthy numerical simulations and facilitating experimentation. It should be emphasized that the scaling laws for such situations postulated by Sun et al. [4] are proven by the self-similar turbulent plume theory used here. Note also that the self-similar solutions for unrestricted boundary layers are frequently and successfully employed in confined situations, for example, wind-tunnel operation, multiple nozzles, and other engineering devices are based on such solutions. Such results are useful to construction and safety engineers who need quick estimates for their designs.

## Conflict of interest

The authors declared that there is no conflict of interest.

## Acknowledgement

This work was supported by the National Research Council of Science & Technology (NST) grant by the Korea government (MSIP) (No. CRC-16-02-KICT). This work was also supported by Advanced Research Center Program (NRF-2013R1A5A1073861) and NRF-2016M1A2A2936760.

## Appendix A. Supplementary material

Supplementary data associated with this article can be found, in the online version, at https://doi.org/10.1016/j.ijheatmasstransfer.2018.12.093.

## References

[1] J. Zhang, J. Ji, R. Huo, H. Yuan, R. Yang, A comparison of simulation and experiment on stack effect in long vertical shaft, J. Fire Sci. 24 (2) (2006) 121–135.
[2] G. Xiao, J. Tu, G. Yeoh, Numerical simulation of the migration of hot gases in open vertical shaft, Appl. Therm. Eng. 28 (5–6) (2008) 478–487.
[3] J. Zhang, W. Lu, R. Huo, R. Feng, A new model for determining neutral-plane position in shaft space of a building under fire situation, Build. Environ. 43 (6) (2008) 1101–1108.
[4] X. Sun, L. Hu, W. Chow, Y. Xu, F. Li, A theoretical model to predict plume rise in shaft generated by growing compartment fire, Int. J. Heat Mass Transf. 54 (4) (2011) 910–920.
[5] R. Harish, K. Venkatasubbaiah, Transport phenomena of turbulent fire spread through compartment connected to vertical shaft in tall building, Fire Saf. J. 61 (2013) 160–174.
[6] D. Qi, L. Wang, R. Zmeureanu, An analytical model of heat and mass transfer through non-adiabatic high-rise shafts during fires, Int. J. Heat Mass Transf. 72 (2014) 585–594.
[7] Y. Chen, X. Zhou, Z. Fu, T. Zhang, B. Cao, L. Yang, Vertical temperature distributions in ventilation shafts during a fire, Exp. Therm Fluid Sci. 79 (2016) 118–125.
[8] D. Qi, L. Wang, R. Zmeureanu, The effects of non-uniform temperature distribution on neutral plane level in non-adiabatic high-rise shafts during fires, Fire Technol. 53 (1) (2017) 153–172.
[9] X. Sun, L. Hu, Y. Li, R. Huo, W. Chow, N. Fong, G.C. Lui, K. Li, Studies on smoke movement in stairwell induced by an adjacent compartment fire, Appl. Therm. Eng. 29 (13) (2009) 2757–2765.
[10] J. Ji, L. Li, W. Shi, C. Fan, J. Sun, Experimental investigation on the rising characteristics of the fire-induced buoyant plume in stairwells, Int. J. Heat Mass Transf. 64 (2013) 193–201.
[11] L. Li, J. Ji, C. Fan, J. Sun, X. Yuan, W. Shi, Experimental investigation on the characteristics of buoyant plume movement in a stairwell with multiple openings, Energy Build. 68 (2014) 108–120.
[12] W. Shi, J. Ji, J. Sun, S. Lo, L. Li, X. Yuan, Influence of fire power and window position on smoke movement mechanisms and temperature distribution in an emergency staircase, Energy Build. 79 (2014) 132–142.
[13] J. Ji, H. Wan, Y. Li, K. Li, J. Sun, Influence of relative location of two openings on fire and smoke behaviors in stairwell with a compartment, Int. J. Therm. Sci. 89 (2015) 23–33.
[14] L. Li, J. Ji, W. Shi, Z. Gao, J. Sun, J. Zhu, A modified turbulent mixing model with the consideration of heat transfer between hot buoyant plume and sidewalls in a closed stairwell, Int. J. Heat Mass Transf. 84 (2015) 521–528.
[15] S. Pope, Turbulent premixed flames, Annu. Rev. Fluid Mech. 19 (1) (1987) 237–270.
[16] W.D. Walton, P.H. Thomas, Y. Ohmiya, Estimating temperatures in compartment fires, in: SFPE Handbook of Fire Protection Engineering, Springer, 2016, pp. 996–1023.
[17] Y. Wang, P. Chatterjee, J.L. de Ris, Large eddy simulation of fire plumes, Proc. Combust. Inst. 33 (2) (2011) 2473–2480.
[18] F. Tang, L. Hu, Z. Qiu, Q. Wang, A global model of plume axial temperature profile transition from axisymmetric to line-source pool fires in normal and reduced pressures, Fuel 130 (2014) 211–214.
[19] X. Zhang, L. Hu, W. Zhu, X. Zhang, L. Yang, Axial temperature profile in buoyant plume of rectangular source fuel jet fire in normal-and a sub-atmospheric pressure, Fuel 134 (2014) 455–459.
[20] H. Oka, Y. Oka, Numerical analysis on plume temperature properties formed above a harmonically oscillating fire source, Fire Saf. J. 88 (2017) 56–66.
[21] B. Morton, G. Taylor, J. Turner, Turbulent gravitational convection from maintained and instantaneous sources, in: Proceedings of the Royal Society of London A: Mathematical, Physical and Engineering Sciences, The Royal Society, 1956, pp. 1–23.
[22] J. Turner, Buoyant plumes and thermals, Annu. Rev. Fluid Mech. 1 (1) (1969) 29–44.
[23] S. Yokoi, Study on the prevention of fire-spread caused by hot upward current, Rep. Build. Res. Inst. 34 (1960) 1–118.
[24] B. Morton, Modeling fire plumes, in: Symposium (International) on Combustion, Elsevier, 1965, pp. 973–982.
[25] G. Heskestad, Luminous heights of turbulent diffusion flames, Fire Saf. J. 5 (2) (1983) 103–108.
[26] W.K. George, R.L. Alpert, F. Tamanini, Turbulence measurements in an axisymmetric buoyant plume, Int. J. Heat Mass Transf. 20 (11) (1977) 1145–1154.
[27] B. McCaffrey, Purely Buoyant Diffusion Flames: Some Experimental Results Final Report, Chemical and Physical Processes in Combustion, The National Institute of Standards and Technology (NIST), Miami Beach, 1979, p. 49.

[28] G. Heskestad, Peak gas velocities and flame heights of buoyancy-controlled turbulent diffusion flames, in: Symposium (International) on Combustion, Elsevier, 1981, pp. 951–960.
[29] H.-C. Kung, P. Stavrianidis, Buoyant plumes of large-scale pool fires, in: Symposium (International) on Combustion, Elsevier, 1982, pp. 905–912.
[30] G. Heskestad, Engineering relations for fire plumes, Fire Saf. J. 7 (1) (1984) 25–32.
[31] J.G. Quintiere, Scaling applications in fire research, Fire Saf. J. 15 (1) (1989) 3–29.
[32] J. Quintiere, B. Grove, A unified analysis for fire plumes, in: Symposium (International) on Combustion, Elsevier, 1998, pp. 2757–2766.
[33] Y.B. Zeldovich, Limiting laws of freely rising convection currents, Zhurnal Eksperimentalnoii Teoreticheskoy Fizika 7 (1937) 1463–1465, The English translation in Y. B. Zeldovich. Selected Works of Ya. B. Zeldovich, vol. 1. Chemical Physics and Hydrodynamics. Limiting laws of freely rising connective currents, Princeton University Press, Princeton, 1992.
[34] Y. Jaluria, Natural Convection: Heat and Mass Transfer, Pergamon, Oxford, 1980.
[35] L.P. Yarin, The Pi-Theorem: Applications to Fluid Mechanics and Heat and Mass Transfer, Springer-Verlag, Berlin, Heidelberg, 2012.
[36] J. Sun, L. Hu, Y. Zhang, A review on research of fire dynamics in high-rise buildings, Theor. Appl. Mech. Lett. 3 (4) (2013) 042001.
[37] H.R. Baum, R.G. Rehm, The equations of motion for thermally driven, buoyant flows, J. Res. Nat. Bur. Stand. 83 (1978) 297–308.
[38] K.B. McGrattan, H.R. Baum, R.G. Rehm, A. Hamins, G.P. Forney, J.E. Floyd, S. Hostikka, K. Prasad, Fire Dynamics Simulator–Technical Reference Guide, National Institute of Standards and Technology, Building and Fire Research Laboratory, 2000.
[39] R. Span, W. Wagner, A new equation of state for carbon dioxide covering the fluid region from the triple-point temperature to 1100 K at pressures up to 800 MPa, J. Phys. Chem. Ref. Data 25 (6) (1996) 1509–1596.
[40] P.E. DesJardin, T.J. O'Hern, S.R. Tieszen, Large eddy simulation and experimental measurements of the near-field of a large turbulent helium plume, Phys. Fluids 16 (6) (2004) 1866–1883.
[41] G. Abramovich, The Theory of Turbulent Jets, MIT Press, Boston, 1963.